

Failure Assessment Diagram for Brazed 304 Stainless Steel Joints

Yury Flom
Goddard Space Flight Center, Greenbelt, MD

The NASA STI Program Office ... in Profile

Since its founding, NASA has been dedicated to the advancement of aeronautics and space science. The NASA Scientific and Technical Information (STI) Program Office plays a key part in helping NASA maintain this important role.

The NASA STI Program Office is operated by Langley Research Center, the lead center for NASA's scientific and technical information. The NASA STI Program Office provides access to the NASA STI Database, the largest collection of aeronautical and space science STI in the world. The Program Office is also NASA's institutional mechanism for disseminating the results of its research and development activities. These results are published by NASA in the NASA STI Report Series, which includes the following report types:

- **TECHNICAL PUBLICATION.** Reports of completed research or a major significant phase of research that present the results of NASA programs and include extensive data or theoretical analysis. Includes compilations of significant scientific and technical data and information deemed to be of continuing reference value. NASA's counterpart of peer-reviewed formal professional papers but has less stringent limitations on manuscript length and extent of graphic presentations.
- **TECHNICAL MEMORANDUM.** Scientific and technical findings that are preliminary or of specialized interest, e.g., quick release reports, working papers, and bibliographies that contain minimal annotation. Does not contain extensive analysis.
- **CONTRACTOR REPORT.** Scientific and technical findings by NASA-sponsored contractors and grantees.

- **CONFERENCE PUBLICATION.** Collected papers from scientific and technical conferences, symposia, seminars, or other meetings sponsored or cosponsored by NASA.
- **SPECIAL PUBLICATION.** Scientific, technical, or historical information from NASA programs, projects, and mission, often concerned with subjects having substantial public interest.
- **TECHNICAL TRANSLATION.** English-language translations of foreign scientific and technical material pertinent to NASA's mission.

Specialized services that complement the STI Program Office's diverse offerings include creating custom thesauri, building customized databases, organizing and publishing research results . . . even providing videos.

For more information about the NASA STI Program Office, see the following:

- Access the NASA STI Program Home Page at <http://www.sti.nasa.gov/STI-homepage.html>
- E-mail your question via the Internet to help@sti.nasa.gov
- Fax your question to the NASA Access Help Desk at (443) 757-5803
- Telephone the NASA Access Help Desk at (443) 757-5802
- Write to:
NASA Access Help Desk
NASA Center for AeroSpace Information
7115 Standard Drive
Hanover, MD 21076

Trade names and trademarks are used in this report for identification only. Their usage does not constitute an official endorsement, either expressed or implied, by the National Aeronautics and Space Administration.

Available from:

NASA Center for AeroSpace Information
7115 Standard Drive
Hanover, MD 21076-1320

National Technical Information Service
5285 Port Royal Road
Springfield, VA 22161

FAILURE ASSESSMENT DIAGRAM FOR BRAZED 304 STAINLESS STEEL JOINTS

ABSTRACT

Interaction equations were proposed earlier to predict failure in Albemet 162* brazed joints. Based on the test results of this study, it was determined that the same interaction equations can be used for lower bound estimate of the failure criterion in 304 stainless steel joints brazed with silver-based filler metals as well as for construction of the Failure Assessment Diagrams (FAD).

1.0 INTRODUCTION

Prediction of failure in brazed joints subjected to complex loading conditions continues to challenge designers and structural analysts attempting to estimate margins of safety in critical assemblies fabricated by brazing. Despite the fact that brazed components and structures are extensively used in the aerospace industry, literature is lacking simple engineering procedures or guidelines for failure assessment of brazed joints.

Earlier work [1] demonstrated that interaction equations could be used for failure assessment of Albemet 162 joints brazed with AWS BAlSi-4 (88%Al, 12%Si) filler metal. In the current effort, different base / filler metal combinations consisting of 304 SS brazed with pure silver and AWS BAg8 (78%Ag, 28%Cu eutectic) filler metals were evaluated.

This memorandum provides information on specimen design, fabrication and testing performed by the Materials Engineering Branch to verify that interaction equations used earlier could also be applied for failure assessment of other brazed systems.

2.0 APPROACH

This effort consisted of two parts. In first part design values of tensile σ_o and shear τ_o strength (allowables) were determined. These allowables were used in interaction equation (1). The purpose of the second part was to verify that this equation can be used as a lower bound FAD for 304SS-silver brazed joints. A semi-empirical interaction equation proposed in [1] is shown below:

$$\frac{\sigma}{\sigma_o} + \frac{\tau}{\tau_o} \leq 1 \quad (1)$$

*- Brush and Wellman trade name for 62%Be 38%Al metal matrix composite

In this equation σ and τ are the maximum normal tensile and shear stresses acting on the filler metal layer in the brazed joint. σ_0 was determined experimentally. Since the shear strength of stainless steel lap joints brazed with silver-based filler metals is a well established quantity [2-4], it was more cost effective to omit fabrication and testing of the lap shear specimens. Instead, it was decided to accept $\tau_0 = 15$ ksi (103.5 mpa). This value is listed as the shear strength allowable in [4].

Equation (1) was validated by testing specially designed brazed specimens. Tensile and shear stresses acting on the brazed joints were calculated using engineering mechanics of materials, as described in Appendix.

3.0 EXPERIMENTAL PROCEDURE

3.1 Test Specimens

All test specimens were fabricated from cold rolled 304SS bars purchased from McMaster Carr. In addition to brazed specimens, several blank tensile specimens were fabricated and tested to compare the properties of the base metal with the properties of the brazed joints. There were two types of specimens designed to subject the brazed joints to a combined action of shear and normal stresses: double scarf and V-type. A total of five different configurations of specimens used in this effort are shown in Figure 1. Fabrication sequence of a double scarf specimen is shown in Fig.2. Figures 3-5 show photographs of various test specimens at different phases of fabrication process.

The double scarf geometry reduces the tendency of specimen to rotate during tensile test. Also, since the double scarf test specimen has two geometrically identical brazed joints and the failure occurs in only one joint, each tested specimen has one brazed joint still intact. This allows for a metallographic examination of the brazed joint that experienced the condition of imminent failure. The V-type specimen geometry [5] eliminates rotation, provides fully axisymmetric loading conditions while subjecting the brazed joint to a combined tension and shear load. Test specimen identifications are explained in Table 1.

Brazing was performed in a vacuum furnace. All specimens were electrologically Ni plated prior to brazing. One set of specimens was brazed using AWS BAg-0 (pure silver) and another set was brazed with BAg-8 (silver-copper eutectic) filler metals. Filler metal foils were preplaced between the faying surfaces. For simplicity, AWS BAg-0 filler metal is referred to in the rest of the text as Ag. Typical time-temperature records of the brazing cycles are shown in Figure 6. After brazing, all specimens were machined into the standard round tensile test coupons, as shown in Fig.5

Table 1. Test Specimen Identification

Spec. ID	What it means
ButtAg-1	Specimen # 1 butt brazed using Ag filler metal
ButtBAg8-1	Specimen # 1 butt brazed using AWS BAg8 filler metal
D60Ag-2	Specimen # 2, double 60° scarf joint, brazed with Ag filler metal
D45BAg8-3	Specimen # 3, double 45° scarf joint, brazed with AWS BAg8 filler metal
V60Ag-1	Specimen # 1, 60° V-shape joint, brazed with Ag filler metal.
304SS-Ag	Base metal tensile coupon exposed to Ag brazing cycle

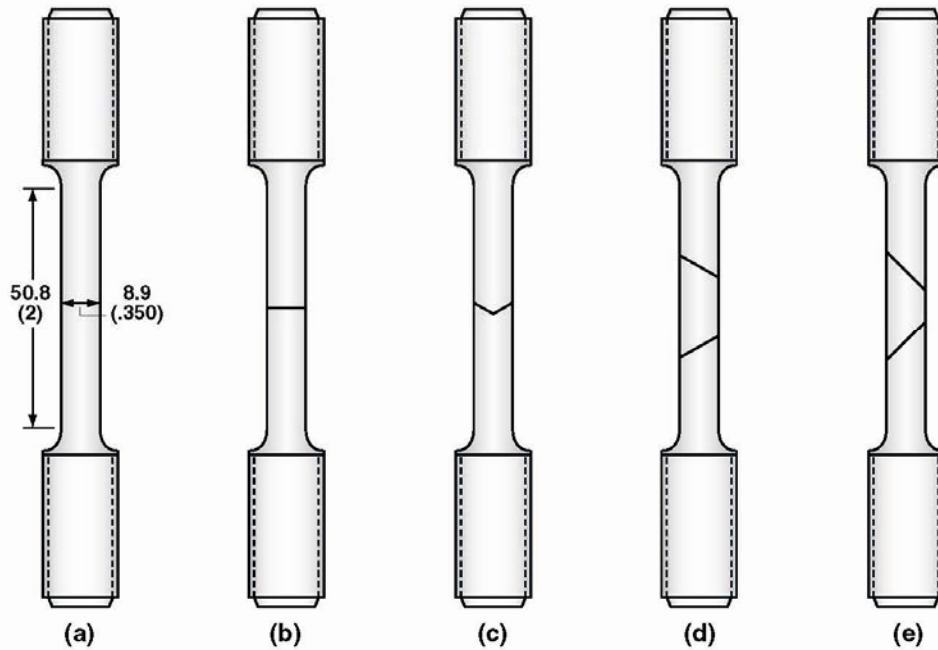


Fig.1 Geometry of the test specimens used in this effort. Base metal blanks (a) were tested to establish the property baseline. Butt brazed (b), V60 (c) and double scarf 60°(d) and 45°(e) were tested to determine the failure loads used to calculate normal and shear stresses at failure acting on the braze layer.

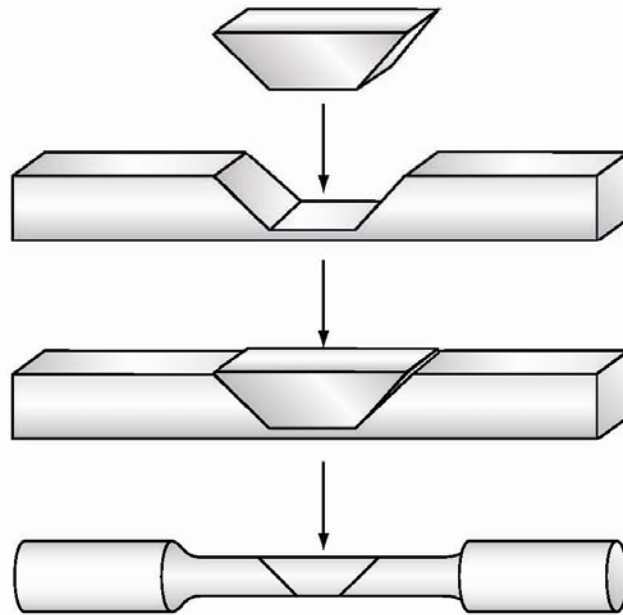


Fig. 2 Showing schematic of scarf specimen fabrication sequence.

3.2 Mechanical testing

All specimens, including the blank ones, were tested on Instron 4115 test frame using a crosshead speed of 0.05 in/min. A 1" gage length extensometer was used to record the elongation of the test specimens. In case of the double scarf specimens, the extensometer was recording the elongation across only one joint. When elongation reached approximately 1%, extensometer was removed to avoid possible exposure to the shock event during brazed joint failure, and the Bluehill 2 testing software continued to acquire the load / displacement record. This feature allows for an uninterrupted plot of the entire test up to the failure point. Figures 7-8 show typical stress-strain curves for all specimens tested in this effort. Prior to tensile testing, the stainless steel blanks were exposed to the same brazing cycle time/temperature conditions as the brazed specimens. Typical appearances of the fractured specimens are shown are Figure 9.

3.3 Metallographic examination

The remaining brazed joints in each 45° and 60° double scarf specimens tested at the highest strength were cross sectioned and metallographically polished, as schematically shown in Figure 10. Metallographic cross sections were examined under optical microscope to observe the condition of the braze filler metal interlayer immediately prior

to fracture. Various microstructural features observed on the metallographic cross sections and discussed in the following section are shown in Figures 11 through 14.

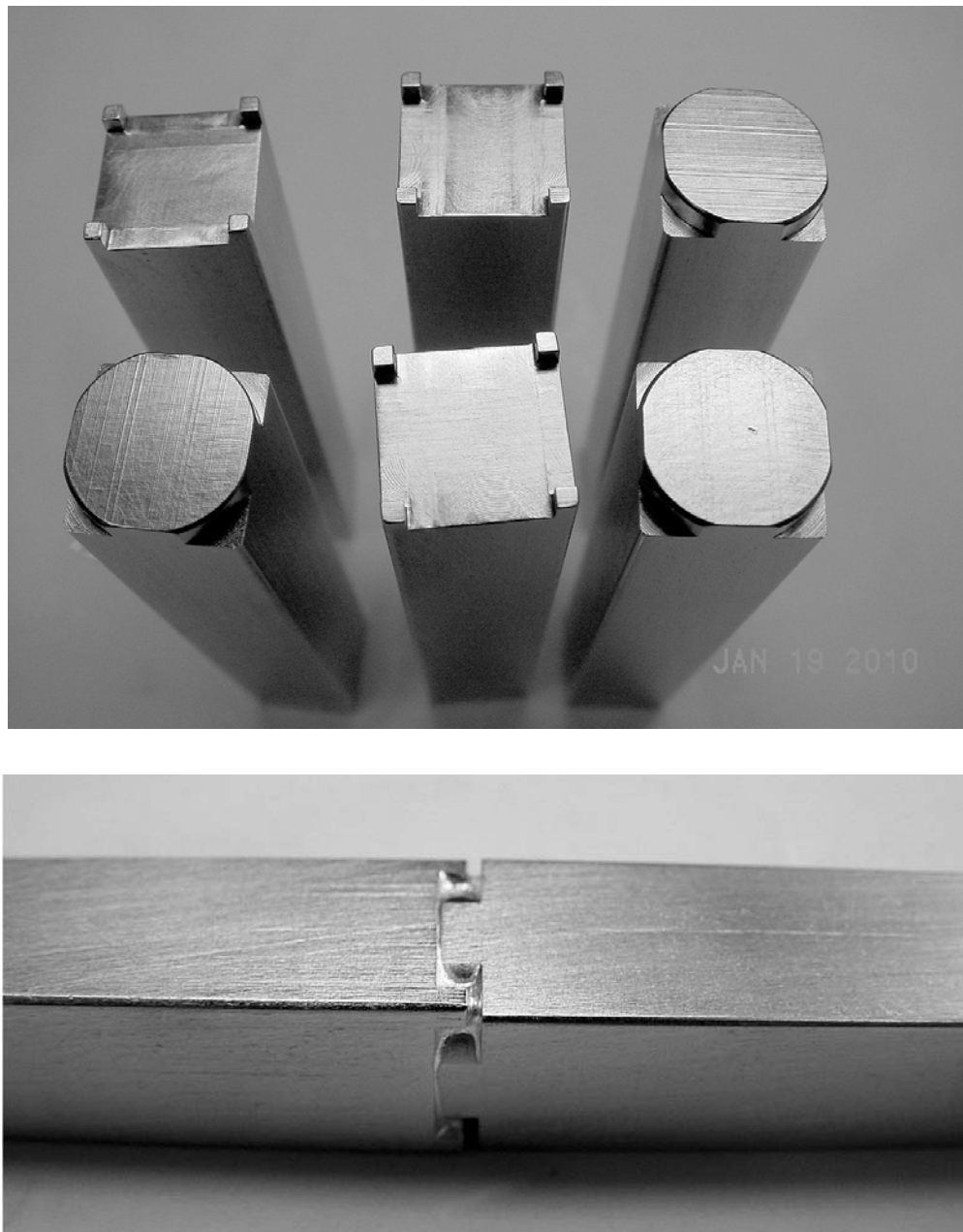


Fig.3. Top view shows the alignment features on the interfaces of male and female halves forming the butt-brazed specimens. These features are similar to the ones suggested in European standard EN 12797 entitled “Brazing-Destructive tests of brazed joints”. The filler metal foil is placed between the interfaces prior to brazing. Bottom view shows as brazed butt joint prior to machining.

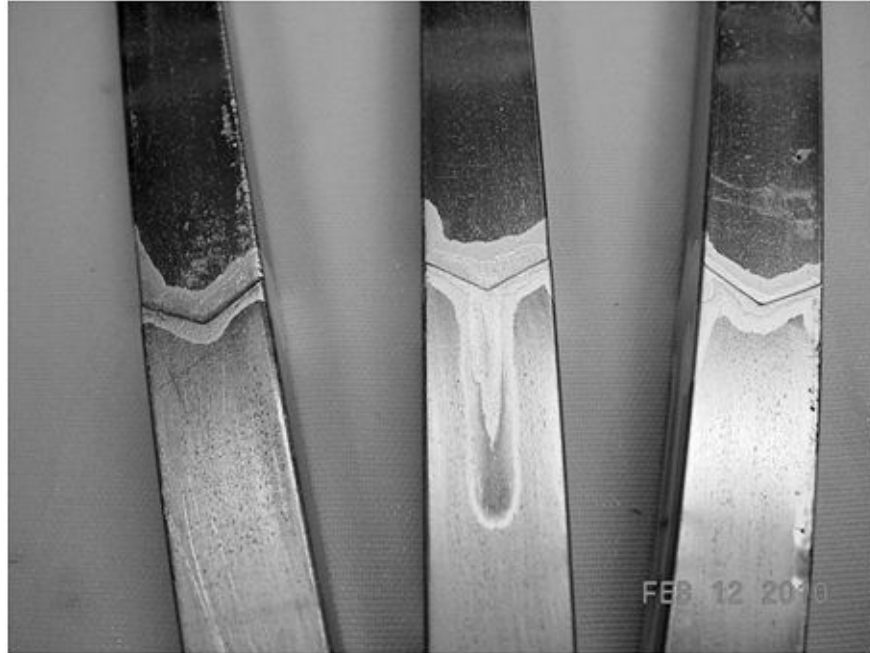


Fig. 4 A close-up of the V60 joints in as-brazed condition.

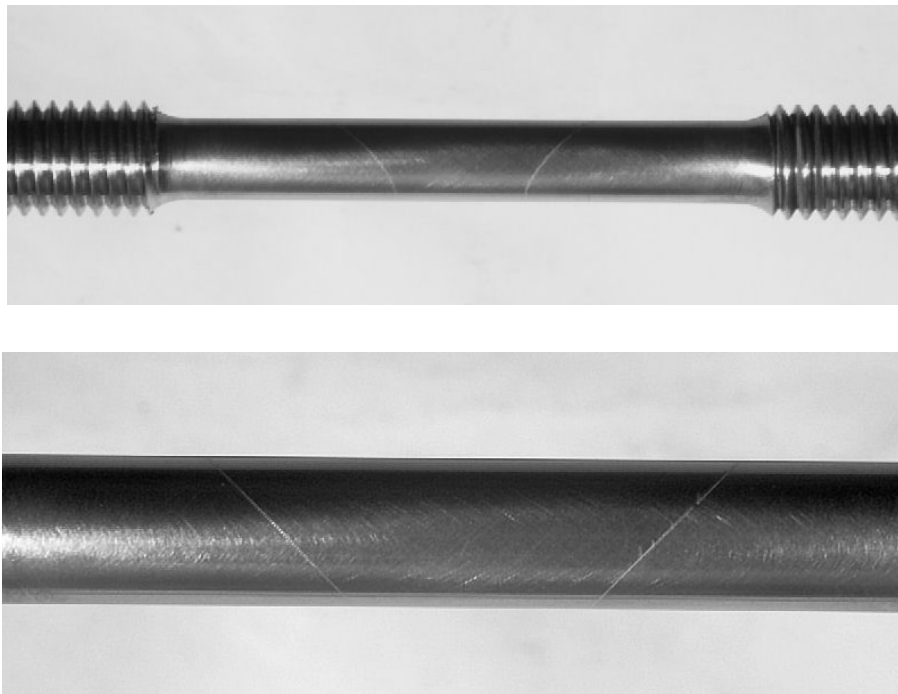


Fig.5. Top view shows one of the D45 type specimens after machining. A close-up view of the brazed joints in the same specimen is shown at the bottom.

4. RESULTS AND DISCUSSION

4.1 Mechanical Testing

As one can see, all specimens brazed with AWS BAg8 filler metal failed at higher loads than their counterparts brazed with pure silver (Fig.7, 8). Two factors are responsible for this difference. One factor is related to the difference in properties between 304SS base metal exposed to two different braze cycles. 304SS is considerably weaker and more ductile after Ag braze cycle than after the BAg8 one. The annealing temperature for 304SS is somewhere between 1010° and 1121°C [6]. Consequently, the Ag brazing cycle (see Fig. 6) brings the 304SS base metal very close to fully annealed condition.

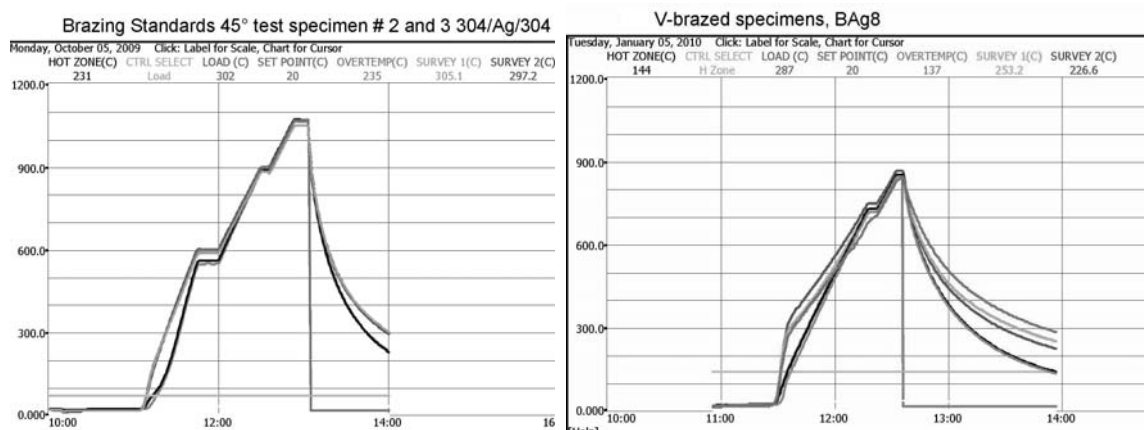
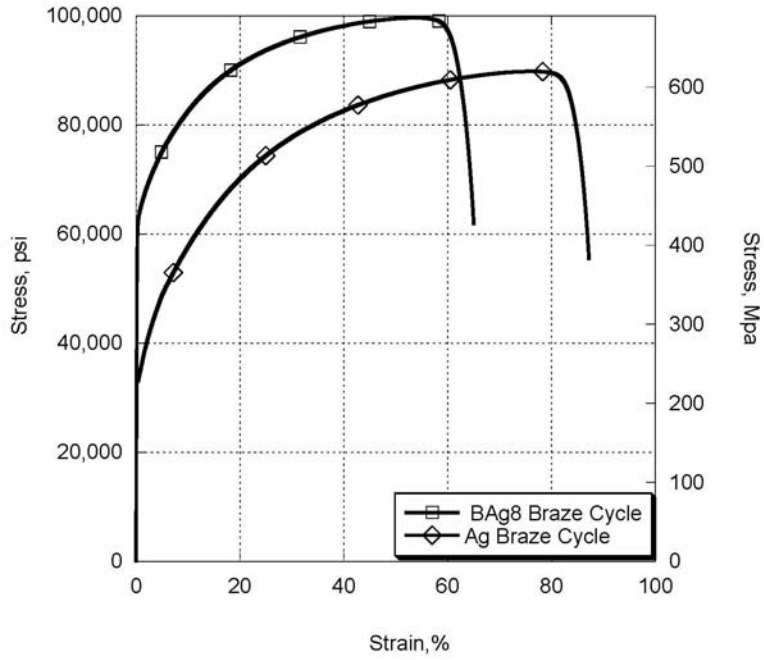


Fig. 6 Brazing cycles for Ag-brazed (left) and BAg8-brazed test specimens.

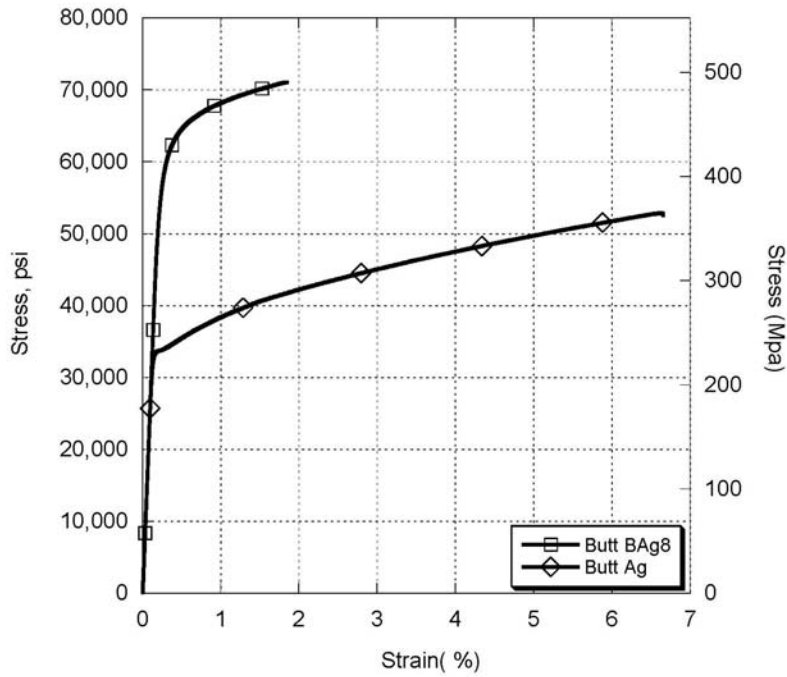
Another factor is related to the difference in strength between Cu-Ag alloy and pure Ag due to solid solution hardening effect. It is expected that the silver-copper alloy (AWS BAg8) would have higher strength than unalloyed silver. For example, tensile strength of annealed silver-copper eutectic is reported somewhere between 40 and 44 ksi (276 – 304 Mpa), whereas typical tensile strength of pure silver is only around 18.2 ksi (130 Mpa) [7,8]. The difference in strength between the joints brazed with AWS BAg8 and Ag filler metals is evident from the engineering tensile stress vs. strain plots shown in Fig.7. For clarity, only the data from the specimens that showed the highest strength are present on the plots. All specimens, regardless of the joint geometry, demonstrated much higher strengths than the strengths of their respective filler metals. This is a well known property of butt brazed joints [9,10]. As one can see from the plots, scarf and V-type brazed joints also behave in a similar manner. As a general observation, Ag-brazed joints displayed higher ductility than their counterparts brazed with silver-copper eutectic with the exception of the 45° double scarf joints, which showed the same ductility

STRESS - STRAIN CURVES FOR 304SS BLANK TENSILE SPECIMENS EXPOSED TO DIFFERENT BRAZING CYCLES



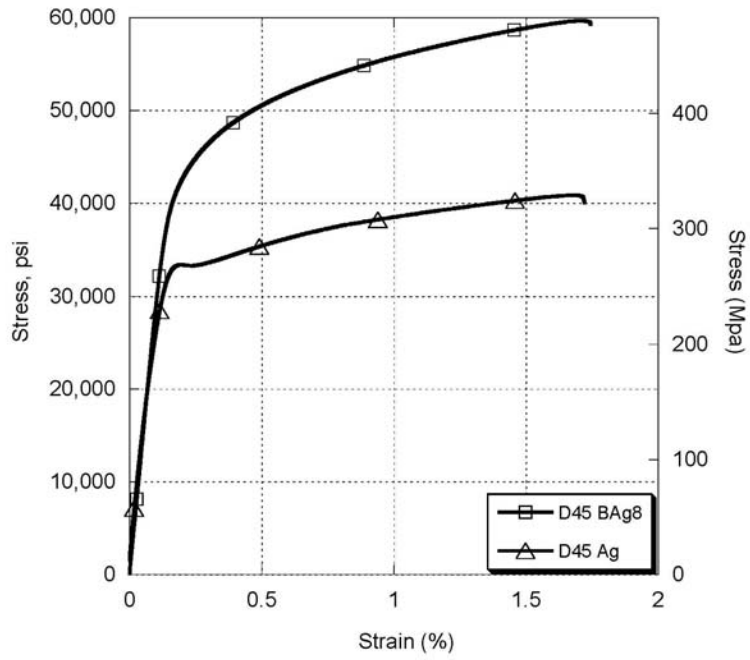
a)

STRESS-STRAIN CURVES FOR BUTT JOINTS BRAZED WITH BAg8 AND Ag FILLER METALS



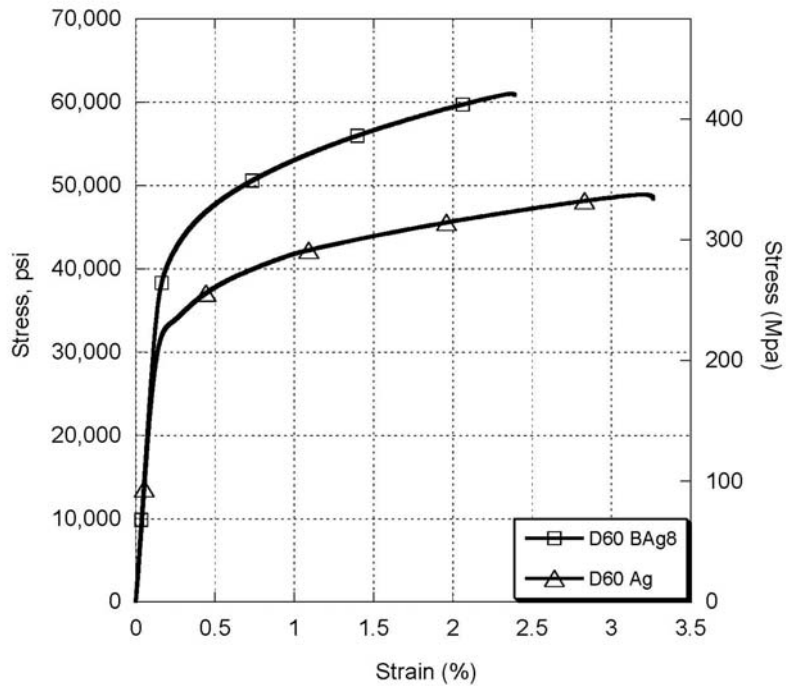
b)

STRESS - STRAIN CURVES FOR DOUBLE SCARF 45° SPECIMENS BRAZED WITH BAg8 AND Ag FILLER METALS

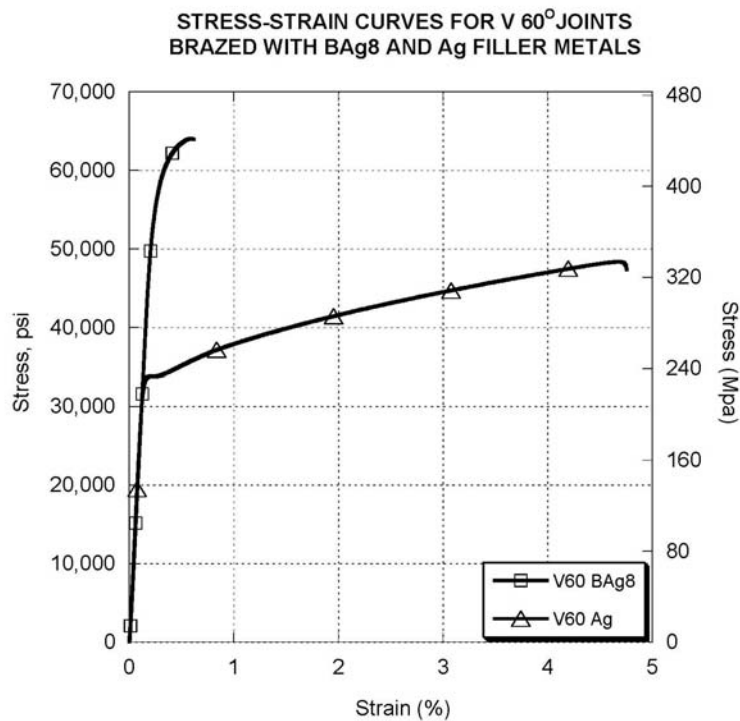


c)

STRESS - STRAIN CURVES FOR DOUBLE SCARF 60° SPECIMENS BRAZED WITH BAg8 AND Ag FILLER METALS



d)



e)

Fig.7. Stress-strain curves comparing BAg8- and Ag-brazed test specimens. All specimens regardless of configuration and brazed with BAg8 filler metal demonstrated higher strength than their pure silver brazed counterparts.

regardless of the filler metal. Fig. 8 shows the same plots grouped in accordance with the filler metal used. Ag-brazed joints essentially follow the deformation behavior of the 304SS base metal. It appears that D60 Ag scarf joints required higher stresses to sustain their plastic deformation compared to the rest of the joints including the base metal. BAg8 – brazed specimens also follow the base metal stress strain curve. In this case, however, the scarf joints yielded earlier than butt- and V-brazed joints as well as the base metal itself. It appears that behavior of the scarf-brazed joints was not consistent in terms of their yield onset. Yielding could occur either below (Fig.8a) or above (Fig.8b) their respective base metals. This observation is most likely due to an experimental artifact caused by a complex interaction between the slip along the braze interfaces and extensometer readout.

Results of all mechanical tests are presented in Table 2. Selection of the brazed joint tensile strength allowable σ_0 was based on test results of butt Ag specimens.

Comparing the test results of the butt joints, BAg8-brazed specimens showed approximately 50% higher strength than their Ag-brazed counterparts. Consequently,

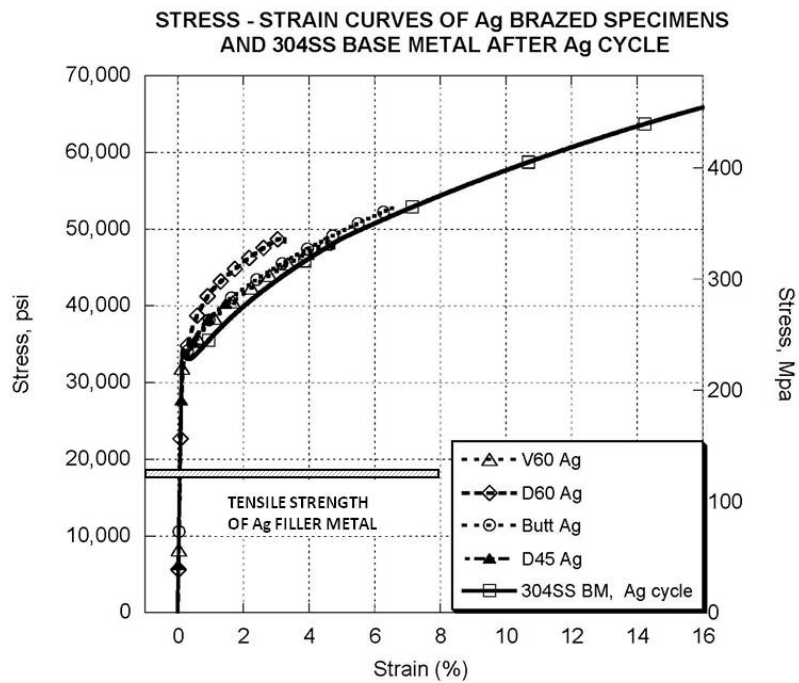
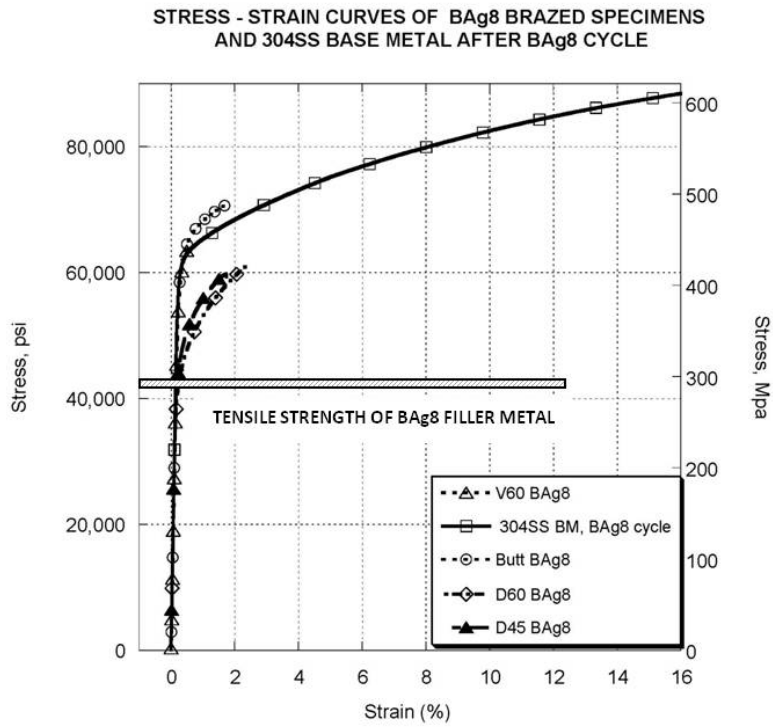


Fig. 8. The same plots as in Fig.7 only grouped according to the AWS BAg8 (a) and Ag (b) filler metals. All specimens demonstrated higher strength than their respective filler metals.

Table 2. Test Results

Spec.ID	Ultimate Tensile Strength* TUS		Normal stress braze plane σ_B		Shear stress braze plane τ_B		Normal stress ratio** R_σ	Shear stress ratio** R_τ
	Ksi	Mpa	ksi	Mpa	ksi	Mpa		
ButtAg-1	53	363	53	366	0	0	1.4	0.0
ButtAg-2	48	332	48	331	0	0	1.3	0.0
ButtAg-3	46	316	46	317	0	0	1.2	0.0
ButtBAg8-1	75	517	75	518	0	0	2.0	0.0
ButtBAg8-2	71	490	71	490	0	0	1.8	0.0
ButtBAg8-3	75	515	75	518	0	0	2.0	0.0
D60BAg8-1	61	420	35	238	20	137	0.9	1.3
D60BAg8-2	61	424	37	254	21	146	1.0	1.4
D60BAg8-3	57	395	34	233	19	134	0.9	1.3
D60Ag-1	46	318	46	316	26	182	1.2	1.8
D60Ag-2	49	335	46	316	26	182	1.2	1.8
D60Ag-3	45	313	43	295	25	170	1.1	1.6
D45Ag-1	41	280	21	141	21	141	0.5	1.4
D45Ag-2	40	274	20	138	20	138	0.5	1.3
D45Ag-3	38	265	19	131	19	131	0.5	1.3
D45BAg8-1	55	377	28	190	28	190	0.7	1.8
D45BAg8-2	59	410	30	204	30	204	0.8	2.0
D45BAg8-3	56	387	28	193	28	193	0.7	1.9
V60Ag-1	48	333	36	248	21	143	0.9	1.4
V60Ag-2	46	319	35	238	20	137	0.9	1.3
V60Ag-3	52	361	39	269	23	155	1.0	1.5
V60BAg8-1	67	462	50	347	29	200	1.3	1.9
V60BAg8-2	64	441	48	331	28	191	1.3	1.8
V60BAg8-3	54	375	41	279	23	161	1.1	1.6
304SS-Ag	90	620						
304SS-BAg8	100	690						

* Determined by dividing maximum load by the initial cross sectional area

** $R_\sigma = \sigma_B / \sigma_0$; $R_\tau = \tau_B / \tau_0$ where $\sigma_0 = 38.4$ ksi (265 Mpa); $\tau_0 = 15$ ksi (103.5 Mpa)

pooling the data would not be statistically justified. Since we are interested in determining the lower bound failure criteria, the logical choice would be to use Ag-brazed butt specimen showing the lowest strength. A simple, 3 sigma statistical analysis was performed to estimate σ_o :

$$\sigma_o = \text{AVG}-3\times\text{SIGMA} = ((48+53+46)/3)-3\times\text{STDEV} = 38.4 \text{ ksi (265 Mpa)},$$

as indicated in the foot note of Table 2. A rationale for selecting shear allowable $\tau_o = 15$ ksi (103.5 Mpa) is provided earlier in Section 2.

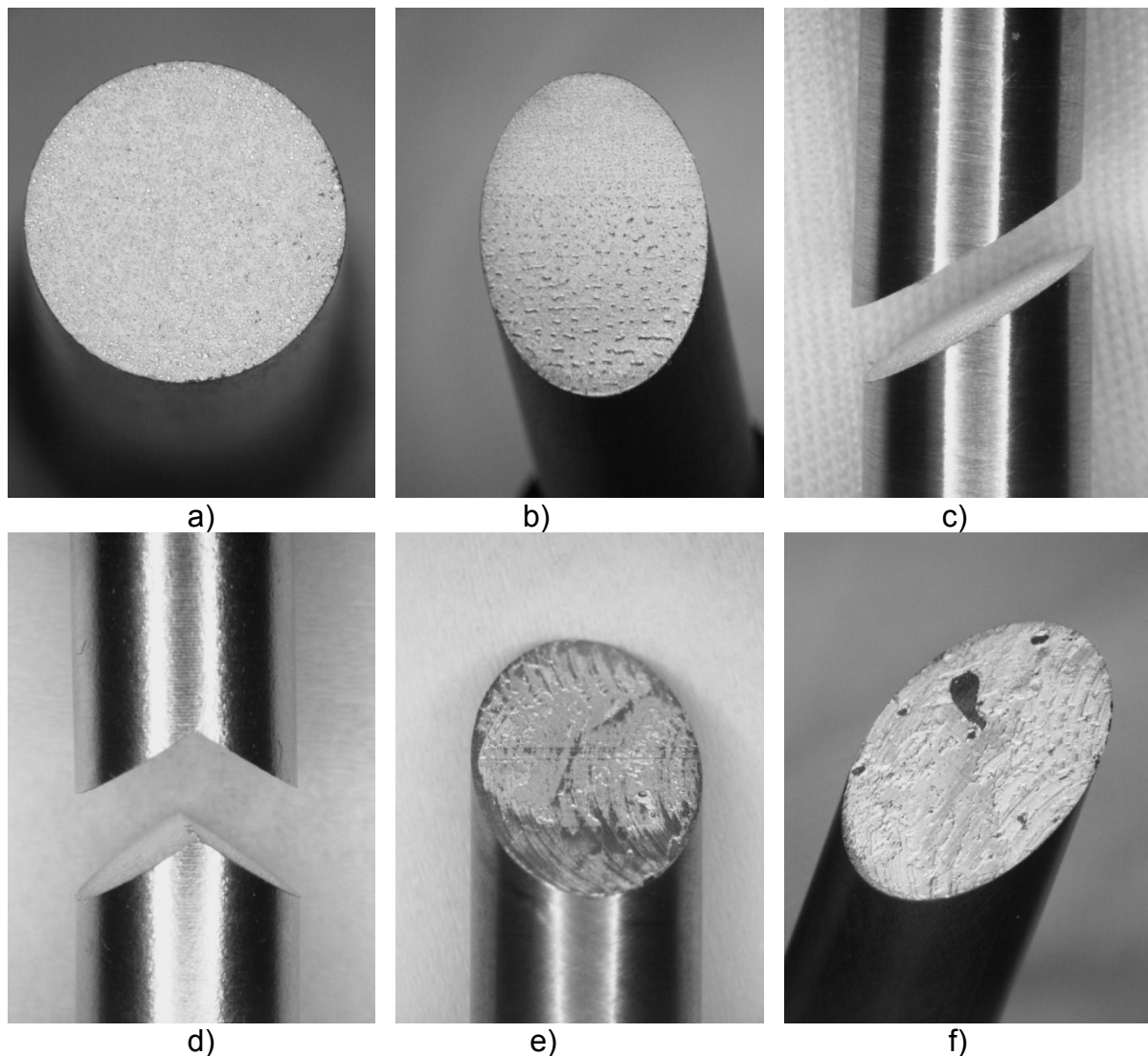
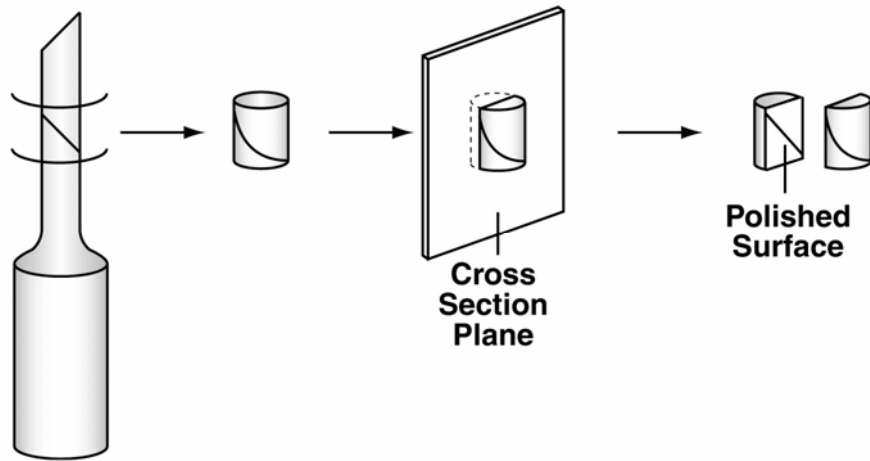


Fig. 9. Shows fracture surfaces of butt (a), scarf (b, c) and v (d) joints after pull test. Some scarf joints, like the ones shown in e) and f), had discontinuity areas that most likely contributed to a reduction in their strength and/or ductility, although no effort was made in this study to correlate a lack of braze with reduction in properties.



a)



b)

Fig. 10. The view (a) is showing metallographic preparation sequence of the scarf joint specimens after mechanical tests. The brazed joint which is still intact (left) is cut from the specimen, cross sectioned and polished. The unetched polished surfaces were examined under optical microscope. Typical polished cross section of 45° scarf joint is shown in view (b).

4.2 Metallographic Examination

Examination of the metallographic cross sections revealed a number of interesting features, as noted below:

- High integrity of the braze layer.

Since the cross sectioned brazed joints were exposed to the failure loads, it was expected to find severe voiding and cracking in the braze layer indicating imminent fracture. However, the microstructures in both Ag- and BAg8-brazed scarf joints appear to be fundamentally sound, showing no evidence of extensive damage such as massive micro-voiding and void linking typically observed in ductile metals immediately prior to failure. The shape and location of the voids found in the braze layers point to their pre-

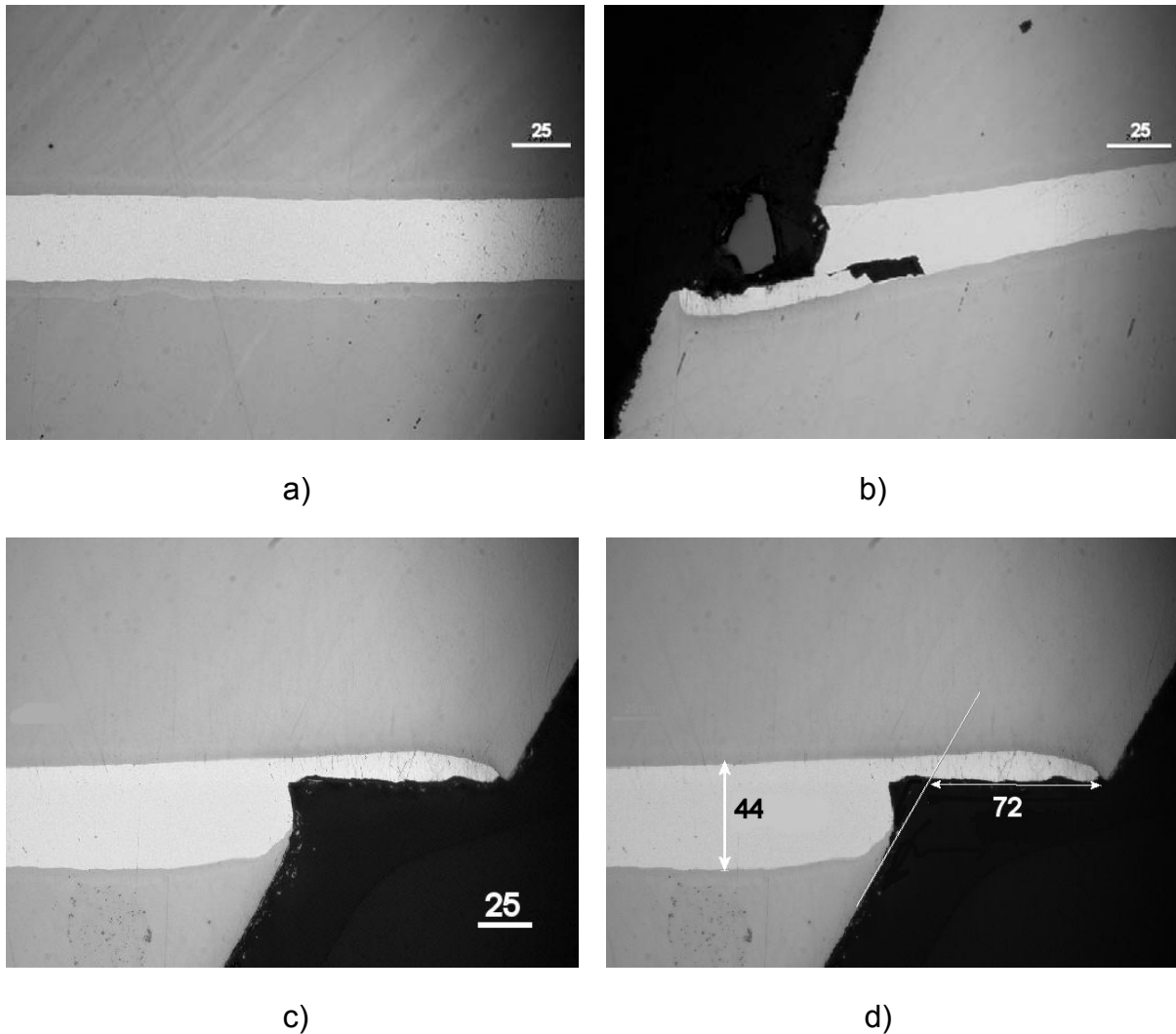


Fig. 11. Images of various locations in the cross section of the D60Ag scarf joint after exposure to failure load. Image (a) is typical. No voids were observed except at the very edge of the joint (b). The shape of the void points to the shear deformation-related origin. Images (c) and (d) show the same edge. Amount of shear strain can be estimated as $72/44 = 164\%$! All dimensions are in microns.

existing nature. It appears that shear plastic deformation of the braze layer resulted in expansion and stretching of pre-existing brazing flaws.

- Uniform shear deformation

Both types of Ag- and BAg8-brazed scarf joints displayed a fairly uniform plastic shear strain along the braze plane. It was very surprising to see typical shear strains in either 45° or 60° scarf joints in excess of 100%! This indicates tremendous resilience of the 304SS/Ag and BAg8-brazed joints and their ability to undergo large plastic deformation

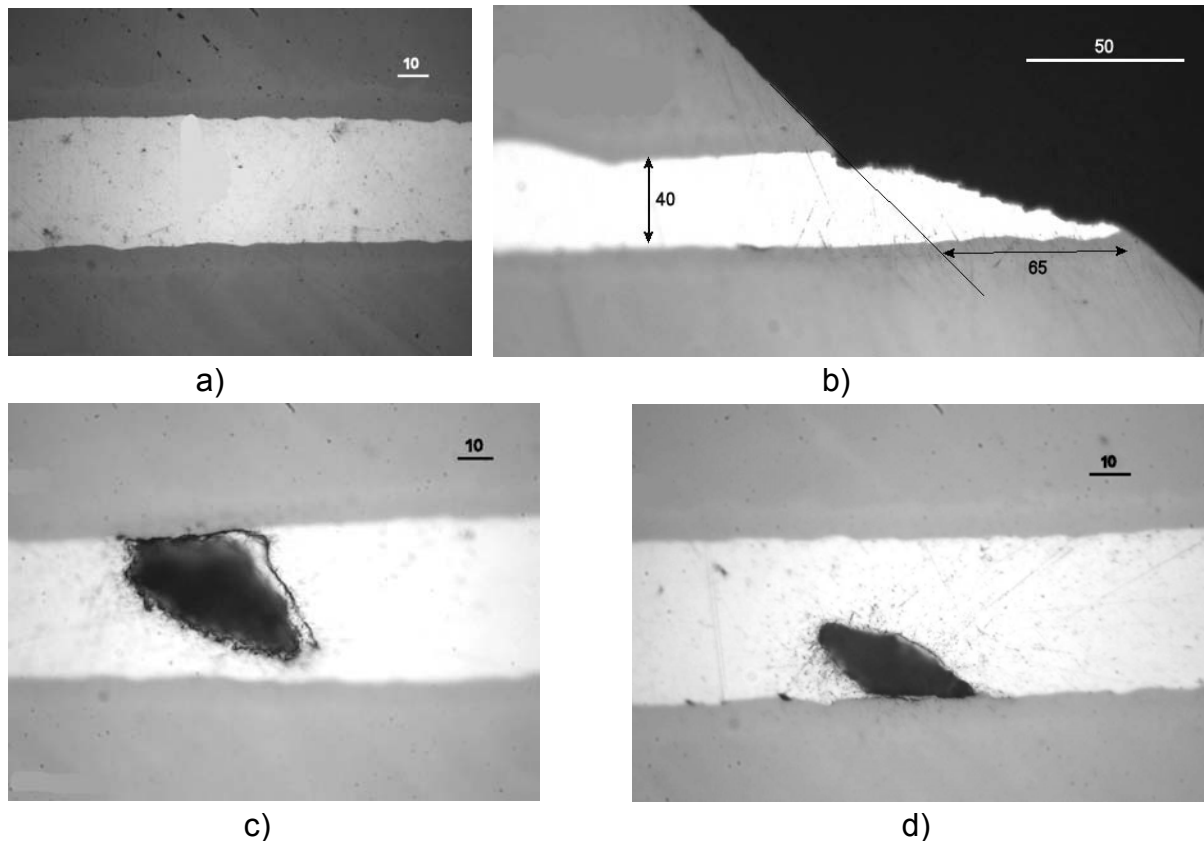


Fig. 12 Cross section of the D45Ag scarf joint. Most of the braze is free from voids and cracks (a). This joint has also experienced very large shear strains (b) that can be estimated as $65/40 = 163\%$. A number of voids could be seen along the braze (c, d). These voids appear to form during brazing and became distorted, tilted and stretched during the pull test. All dimensions are in microns.

prior to failure. A uniform shear strain within the braze layer may also be indicative of the end-to-end uniformity of von Mises stress in the scarf brazed joints tested in this effort. This can be explained by the small aspect ratios (length of the brazed interface divided by the specimen diameter) of 60° and 45° scarf joints. These ratios are $1/\cos 30^\circ$ and $1/\cos 45^\circ$ or 1.15 and 1.41 respectively. These values are very close to the aspect ratio of 1 for the lap shear joints having overlap length equal to the thickness of the base metal T . Such joints are commonly referred to as having $1T$ overlap. Stress analysis of stainless steel lap joints brazed with silver filler metal showed that von Mises stress distribution within $1T$ joints was also quite uniform [3]. Such similarity between scarf joints and lap shear joints indicates that behavior of the 45° and 60° scarf joints is dominated by shear. This is consistent with earlier observations of the behavior of the scarf joints for different base metal / filler metal combinations [5].

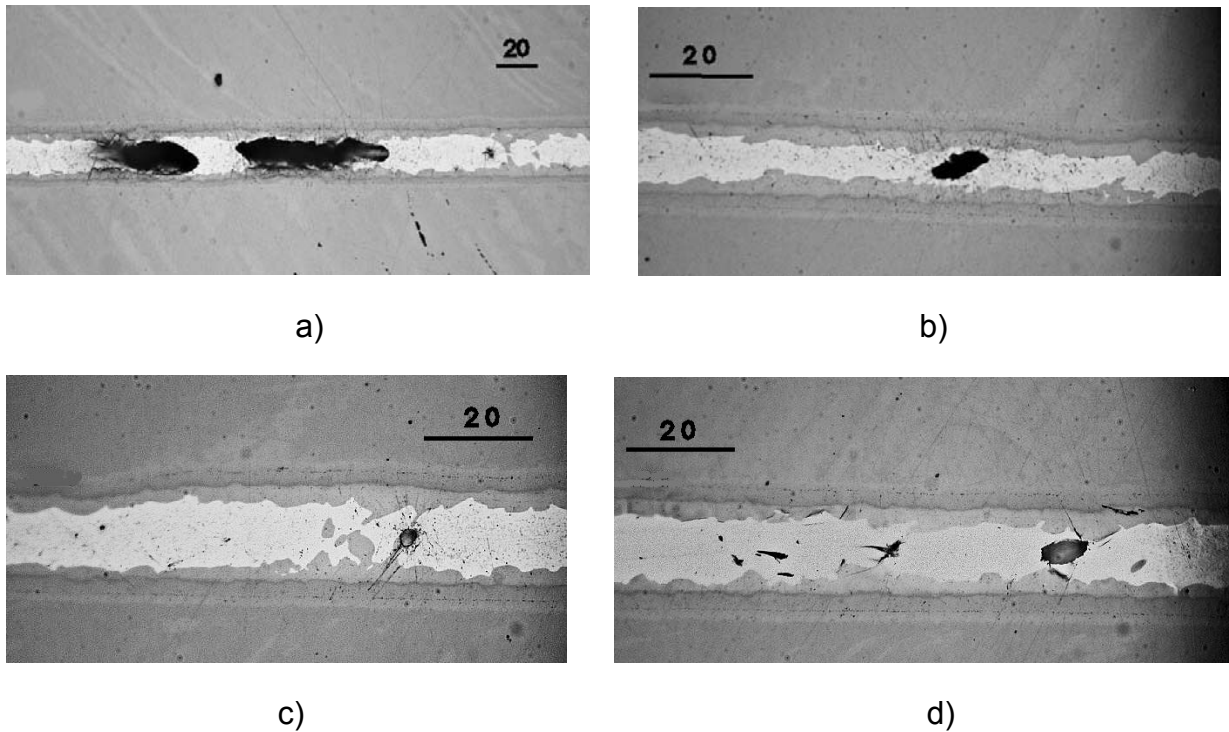


Fig. 13. Cross section of D60BAG8 scarf joint showing more voids. Judging from the shape of these voids, it appears that majority are pre-existing braze defects (a-c) that became deformed during tensile test. Some of the voids, however, were most likely caused by fracture of the filler metal (d). Note that the copper rich phase is tilted during shear deformation within the filler metal. The amount of this tilt or shear strain is fairly uniform from end-to-end of the brazed joint. All dimensions are in microns.

- Benefit of multiphase system

A comparison between the BAg8 and Ag metallographic cross sections in 45° and 60° scarf joints illustrates that a two phase microstructure in BAg8-brazed joints is a much better indicator of the plastic flow than a relatively featureless structure of the silver interlayer. It is evident how the copper-rich phase aligns itself with the shear flow pattern, see Figs. 13 -14. These uniform tilt patterns suggest end-to-end uniformity of shear strain and shear stresses in the scarf joints. Consequently, a ductile multiphase structure is very useful in studying plastic deformation in brazed joints.

4.3 Failure Assessment Diagram (FAD)

Stress ratios presented in Table 2 are plotted in Fig.15. All Ag-brazed joints are denoted by solid symbols and all BAg8-brazed joints are shown with open symbols. A line connecting points with coordinates (1, 0) and (0, 1) represents interaction equation (1) or

$R_{\sigma} + R_{\tau} = 1$, where $R_{\sigma} = \sigma_B / \sigma_0$ and $R_{\tau} = \tau_B / \tau_0$ are tensile and shear stress ratios.

It is quite clear that this line is very conservative and quite adequate to be used as lower bound FAD even for 304SS brazed with pure silver. All BAg8-brazed joints tested higher than the Ag-brazed ones and, therefore, are located further away from the FAD line. Since it is fairly safe to say that pure silver has the lowest strength among the rest of the high temperature silver-based filler metals, it can be concluded that interaction equation

$$R_{\sigma} + R_{\tau} = 1$$

can be used as lower bound FAD for 304SS brazed with high temperature silver-based filler metals.

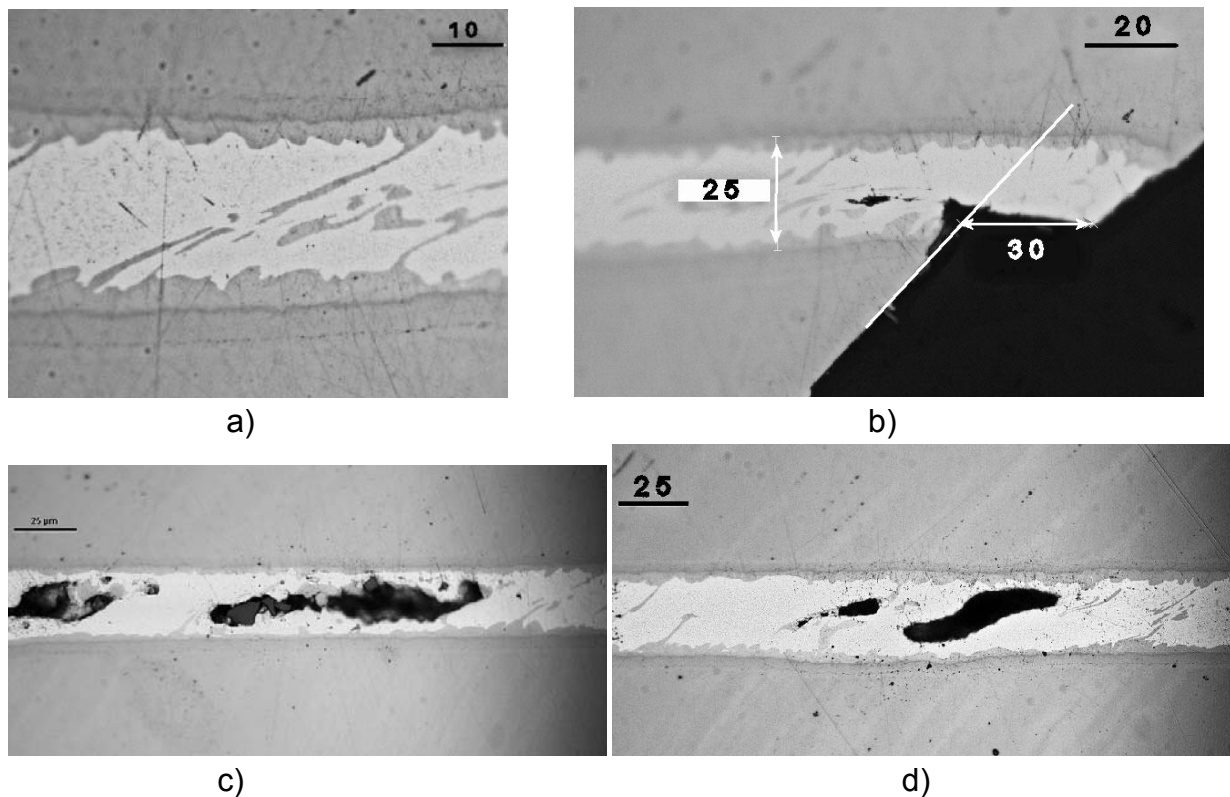


Fig.14 Shows typical (a) optical image of the brazed joint region in tested D45BAg8 specimen as well as the brazed joint edge (b). Extent of plastic deformation can be ascertained from the shear strain estimated as $30/25 = 120\%$. A copper-rich second phase is tilted by the shear deformation in the filler metal. The angle of this tilt is the same from end-to-end which indicates shear strain uniformity within the brazed joint. Most of the voids seem to be related to pre-existing brazing flaws (c, d). All dimensions are in microns.

FAILURE ASSESSMENT DIAGRAM

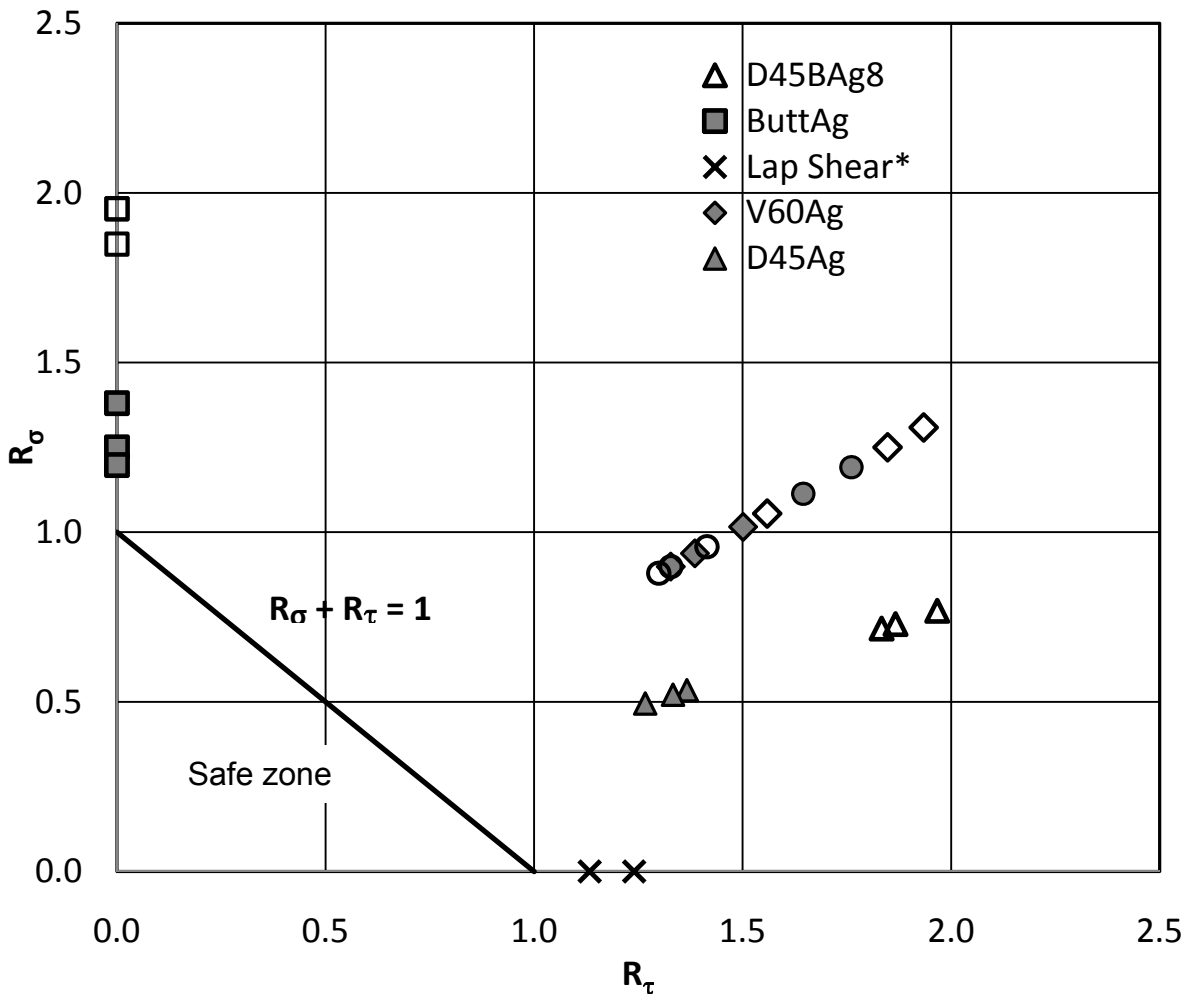


Fig.15 Plot of the stress ratios at failure for all tested specimens. Lap shear test results from the previous investigations [2,3] are marked with "x" and denoted with asterisk in the legend. As one can see all experimental results are located noticeably far away from the lower bound FAD. Consequently, the region inside the FAD line can be considered a "safe" zone.

Acknowledgments

The author would like to thank D. Thomas of D&L Engineering for machining the test specimens as well as D. Puckett, M. Powell and D. Kolos, NASA GSFC, for their assistance in performing mechanical testing, metallographic examination and technical editing. Special thanks go to Mr. Thomas Deming, ATK, for his technical comments. The author also would like to thank Dr. G. Alcorn, NASA GSFC, for sponsoring this effort.

Appendix

Stresses acting on the plane of the brazed joints were hand calculated using engineering mechanics. Figure 16 shows forces acting on the portion of the tensile test specimens adjacent to the brazed joint.

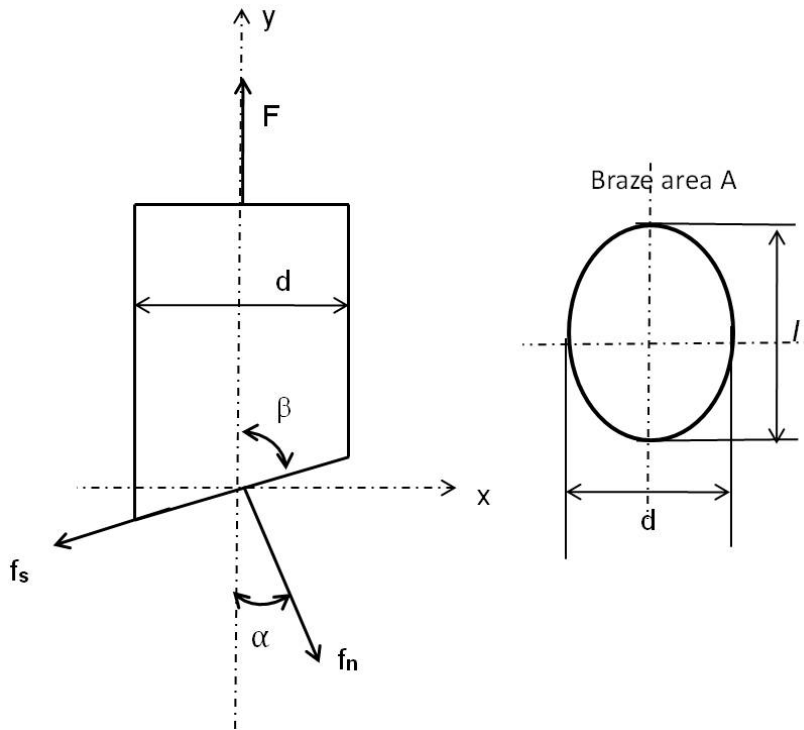


Fig. 16 Force equilibrium diagram used to estimate normal and shear stresses acting on the braze plane.

From equilibrium conditions we can write:

- 1) $f_n \cdot \cos\beta - f_s \cdot \cos\alpha = 0$ along X axis and
- 2) $F - f_s \cdot \sin\alpha - f_n \cdot \sin\beta = 0$ along Y axis, $\alpha + \beta = 90^\circ$

Solving these equations for f_n and f_s will result in:

$$f_n = F \cdot \cos\alpha = F \cdot \sin\beta \text{ and } f_s = F \cdot \sin\alpha = F \cdot \cos\beta$$

Average normal and shear stresses acting on brazed joint can be estimated as:

$\sigma_b = f_n / \text{Braze area}$ and $\tau_b = f_s / \text{Braze area}$. Braze area is an ellipse. Its area equals to: Braze area $A = (\pi \cdot d \cdot l) / 4$, where l can be calculated as $d / \sin\beta$; For example, for D60Ag-1 joint that failed at $F=4432$ lbs (19700 N); $\beta = 60^\circ$ we get:
 $\sigma_b = (4432 \cdot \sin 60^\circ) / ((3.14 \cdot 0.350 \cdot (d / \sin 60^\circ)) / 4) = 35$ ksi (242 Mpa).

References

1. Flom, Y., Wang, L., Powell, M. M., Soffa, M. A., and Rommel, M. L., 2009. Evaluating Margins of Safety in Brazed Joints, *Welding Journal*, 88(10): 31-37.
2. Bredzs, N, and Miller, F., 1968. Use of the AWS standard shear test method for evaluating brazing parameters. *Welding Journal*, 47(11): 481-s to 496-s.
3. Flom, Y., Wang, L., 2004, Flaw Tolerance in Lap Shear Brazed Joints-Part 1. *Welding Journal*, 83(1): 32-s to 38-s.
4. Metallic Materials Properties Development and Standardization (MMPDS), April 2005
5. Peaslee, R.L., The Brazing Test Specimen – Which One? *Welding Journal* 55(10): 850-858
6. Carpenter Stainless Steels – Selecting Alloy Data Fabrication, Carpenter Technology Corporation 2/87/15M, 1987
7. Metals Handbook, 9th edition, Vol.2, ASM, 1979
8. H.E. Cline and D. Lee, “Precious Metals: Science and Technology”, The International Precious Metals Institute, 1991, p.645
9. Handy & Harman, “Easy-Flo and Sil-Fos” Bulletin 20, 1950, p.8
10. Brazing Handbook, 5th edition, AWS, 2007

REPORT DOCUMENTATION PAGE

*Form Approved
OMB No. 0704-0188*

The public reporting burden for this collection of information is estimated to average 1 hour per response, including the time for reviewing instructions, searching existing data sources, gathering and maintaining the data needed, and completing and reviewing the collection of information. Send comments regarding this burden estimate or any other aspect of this collection of information, including suggestions for reducing this burden, to Department of Defense, Washington Headquarters Services, Directorate for Information Operations and Reports (0704-0188), 1215 Jefferson Davis Highway, Suite 1204, Arlington, VA 22202-4302. Respondents should be aware that notwithstanding any other provision of law, no person shall be subject to any penalty for failing to comply with a collection of information if it does not display a currently valid OMB control number.

PLEASE DO NOT RETURN YOUR FORM TO THE ABOVE ADDRESS.

1. REPORT DATE (DD-MM-YYYY) 09-06-2011		2. REPORT TYPE Technical Memorandum		3. DATES COVERED (From - To)	
4. TITLE AND SUBTITLE Failure Assessment Diagram for Brazed 304 Stainless Steel Joints				5a. CONTRACT NUMBER	
				5b. GRANT NUMBER	
				5c. PROGRAM ELEMENT NUMBER	
6. AUTHOR(S) Yury Flom				5d. PROJECT NUMBER	
				5e. TASK NUMBER	
				5f. WORK UNIT NUMBER	
7. PERFORMING ORGANIZATION NAME(S) AND ADDRESS(ES) Goddard Space Flight Center Greenbelt, MD 20771				8. PERFORMING ORGANIZATION REPORT NUMBER	
9. SPONSORING/MONITORING AGENCY NAME(S) AND ADDRESS(ES) National Aeronautics and Space Administration Washington, DC 20546-0001				10. SPONSORING/MONITOR'S ACRONYM(S) NASA	
				11. SPONSORING/MONITORING REPORT NUMBER TM-2011-215876	
12. DISTRIBUTION/AVAILABILITY STATEMENT Unclassified-Unlimited, Subject Category: 31 Report available from NASA Centerfor Aerospace Information, 7115 Standard Drive, Hanover, MD 21076. (443) 757-5802					
13. SUPPLEMENTARY NOTES					
14. ABSTRACT Interaction equations were proposed earlier to predict failure in Albemet 162 brazed joints. Present study demonstrates that the same interaction equations can be used for lower bound estimate of the failure criterion in 304 stainless steel joints brazed with silver-based filler metals as well as for construction of the Failure Assessment Diagrams (FAD).					
15. SUBJECT TERMS Brazing, Structural Analysis, Interaction Equations, Failure Assessment Diagrams					
16. SECURITY CLASSIFICATION OF:			17. LIMITATION OF ABSTRACT	18. NUMBER OF PAGES	19a. NAME OF RESPONSIBLE PERSON
a. REPORT	b. ABSTRACT	c. THIS PAGE			Yury Flom
Unclassified	Unclassified	Unclassified	Unclassified	21	19b. TELEPHONE NUMBER (Include area code) (301) 286-3274

